catalysts

MDPI

Article

Peptide–Gold Nanoparticle Conjugates as Artificial Carbonic Anhydrase Mimics

Dorian J. Mikolajczak and Beate Koksch *

Department of Biology, Chemistry and Pharmacy, Institute of Chemistry and Biochemistry, Freie Universität Berlin, 14195 Berlin, Germany; mikolajd@zedat.fu-berlin.de

* Correspondence: beate.koksch@fu-berlin.de; Tel.: +49-30-838-55344

Received: 24 September 2019; Accepted: 27 October 2019; Published: 29 October 2019

Abstract: We herein describe the design and synthesis of a catalytically active peptide–gold nanoparticle conjugate (Pep-Au-NP) that binds Zn(II) within its peptide monolayer and develops carbonic anhydrase activity. Specifically, a modified variant of the β-sheet forming IHIHIQI-peptide (IHQ), which forms an interstrand 3-His Zn(II)-binding site, was used as a ligand for spherical gold nanoparticles (Au-NPs). The resulting immobilized peptide maintains its ability to form β-sheets, as determined by circular dichroism (CD)-spectroscopy and, thus, maintains its ability to form Zn(II)-binding sites. The addition of Zn(II)-ions to the peptide–gold nanoparticle conjugates (Au@IHQ-NP) resulted in significant improvements in rates of ester hydrolysis of 4-nitrophenyl acetate (4-NPA) and the hydration of CO_2 compared to the unconjugated peptide variants. Recycling of the catalyst revealed that Au@IHQ-NP remains intact with at least 94% of its initial activity after five rounds of CO_2 hydration. The herein reported results reveal that Pep-Au-NPs are able to perform reactions catalyzed by natural metalloenzymes and open up new possibilities for the implementation of these conjugates.

Keywords: catalytically active peptides; gold nanoparticle; carbonic anhydrase mimic; artificial enzymes; catalysis

1. Introduction

The development of nanostructures that mimic the remarkable functions and catalytic properties of natural enzymes, i.e., to create nanozymes [1,2], has been an exciting topic in the field of nanotechnology for the last two decades [3]. Among several approaches used to create nanozymes [4,5], the self-assembly of thiolated ligands onto the surface of gold nanoparticles (Au-NPs) to obtain monolayer-protected gold clusters (Au-MPCs) has emerged as a powerful strategy [6]. In particular, the conjugation of peptides on to the surface of gold nanoparticles to yield peptide–gold nanoparticle conjugates (Pep-Au-NPs) expanded the possibilities for the design of artificial enzymes [7–10]. Peptides are available at low cost by solid-phase peptide synthesis, and their modular design paired with the available repertoire of natural and non-natural amino acids allows for facile diversification of functional groups, and thus the resulting catalytic activities and substrate specificities of the peptide shell. The conjunction of peptides and Au-NPs leads to dense peptide monolayers in which new hydrogen bond and/or charge interactions between individual peptides are established. This enables known enzyme-like effects, such as the perturbation of pK_a values of functional groups and cooperativity in substrate binding [9,11], and can even lead to new catalytic mechanisms [7,8]. Altogether, these effects can greatly improve the catalytic performance of a conjugated versus an unconjugated peptide.

To date, the design and application of Pep-Au-NPs have been limited to organic esterase chemistry, in which catalysis is mediated by a His-imidazole [7–11]. Considering the fact that zinc metalloenzymes perform numerous other types of reactions in nature, including phosphodiester

and amide hydrolysis as well as the (de)hydrogenation of alcohols [12,13], it is of great interest to reconstitute such transformations in vitro by developing appropriate robust synthetic systems. For example, carbonic anhydrase (CA) is a naturally occurring zinc metalloenzyme that efficiently and reversibly catalyzes the hydration of CO_2 into hydrogen carbonate (HCO_3^-). Its high activity originates from its zinc (Zn(II)) containing active site, in which three histidine imidazole moieties coordinate a Zn(II)-ion leaving a vacant space for the association of a water molecule. Zn(II) lowers the pK_a of the bound water and forms a highly nucleophilic hydroxide species which reacts with CO_2, bound in close proximity, to yield HCO_3^- [14]. CA isoforms have been extensively studied due to their clinical importance as drug targets and artificial lungs [15], and their great potential as catalysts in carbon capture systems [16–18]. Especially the latter application drove our interest, as the emission of CO_2 and the associated anthropogenic climate change steadily proceeds and new approaches for the absorption of CO_2 become increasingly urgent. In order to further increase our understanding of the design of Pep-Au-NPs, and to present a new approach for the absorption CO_2, we herein describe the design and synthesis of the first Pep-Au-NP metalloenzyme mimicking carbonic anhydrase activity.

2. Results and Discussion

2.1. Peptide Design

The chosen peptide was designed according to the minimalistic β-sheet-forming heptapeptide IHIHIQI (IHQ) consisting of alternating hydrophobic residues and His ligands in positions i and i + 2 as reported by Rufo et al. [19]. The peptide assembles into extended parallel amyloid β-structures in which three His ligands form an interstrand 3-His Zn(II)-binding site (Figure 1, green) that functions as a hydrophobic primary coordination sphere, analogous to the active site of CA [20].

Grafting of IHQ or its cysteine-containing variant onto Au-NPs leads to irreversible aggregation and precipitation of the resulting Pep-Au-NPs. Thus, IHQ was modified as follows to obtain colloidal stable Pep-Au-NPs. The *N*-terminus was elongated by a spacer sequence of 9 amino acids comprised of Cys, Gly, Ala, and chromogenic Tyr (NH_2-CAGYGAGAG-) to prevent aggregation of the Pep-Au-NPs by steric hindrance between the extended peptide chains and to enable conjugation to the gold-surface by stable S-Au-bonds. The C-terminus was elongated by a peptide sequence comprising the polar amino acids Thr, Gln, and Lys (-GTQK), which are residues found in the secondary coordination sphere of CA, for two reasons: first, positively charged Lys residues increase the electrostatic stabilization of the peptide monolayer by Coulomb repulsion between individual peptide chains; second, this sequence introduces a polar region that potentially assists in the catalytic process by engaging in stabilizing interactions with the transition state, or by providing a region which facilitates the release of product and/or solvent exchange [20,21]. The *C*-terminus was amidated to prevent possible aggregation of Pep-Au-NP after the addition of Zn(II).

The fully modified peptide sequence, referred to as IHQ-NP (Figure 1), was directly applied as a stabilizing agent in the reduction reaction of $HAuCl_4$ by $NaBH_4$. The obtained bench stable Pep-Au-NPs are referred to as Au@IHQ-NP. The synthesized spherical Au@IHQ-NP possess a mean diameter of 10.8 ± 2.8 nm, which was determined by transmission electron microscopy (TEM, Supplementary Materials). Successful conjugation of IHQ-NP to the Au-NPs was verified by FT-IR-spectroscopy (Supplementary Materials). FT-IR stretching frequencies of characteristic bands of the peptide, including the Amide A, Amide I, and Amide II band, are present within the IR-spectrum of Au@IHQ-NP, confirming the presence of bound IHQ-NP. Characterization by UV/vis-spectroscopy (Supplementary Materials) shows a single surface plasmon resonance maximum at 525 nm, which is characteristic for spherical Au-NP. By applying supernatant analysis, the mean peptide loading per nanoparticle was determined to be 859 peptides/Au-NP. This corresponds to an average peptide density of 2.26 pep/nm^2, which is consistent with literature reported peptide densities in the range of 1.41–2.55 pep/nm^2, depending on the peptide length [9,11,22,23].

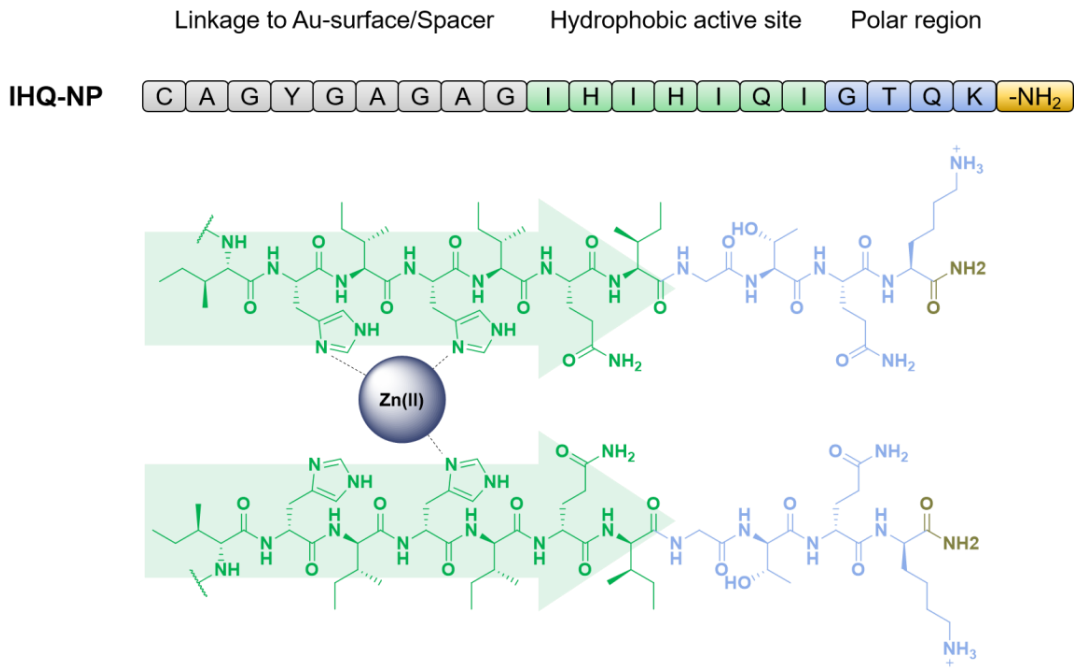

Figure 1. (Top) Peptide sequence of designed and studied IHQ-NP and (bottom) structures of the polar region (blue) and hydrophobic segment (green) of IHQ-NP and the corresponding 3 His Zn(II)-center formed by interstrand interactions between two individual β-sheet forming IHQ-NP peptides (green arrow).

As the formation of β-sheets is a prerequisite for the generation of the 3-His Zn(II)-binding site, and thus the successful coordination of Zn(II) [19], circular dichroism (CD) spectroscopy was performed in order to assess the secondary structure of (un)conjugated IHQ-NP and its Zn(II)-dependency.

The CD-spectra of IHQ-NP and Au@IHQ-NP show zinc-independent single ellipticity minima around 215 nm, respectively, which is characteristic for β-sheet structures (Figure 2). Hence, IHQ-NP and conjugated IHQ-NP maintain the ability to form β-sheet structures even when immobilized at the surface of Au-NPs, indicating the presence of functional Zn(II)-binding domains and potential catalytic sites.

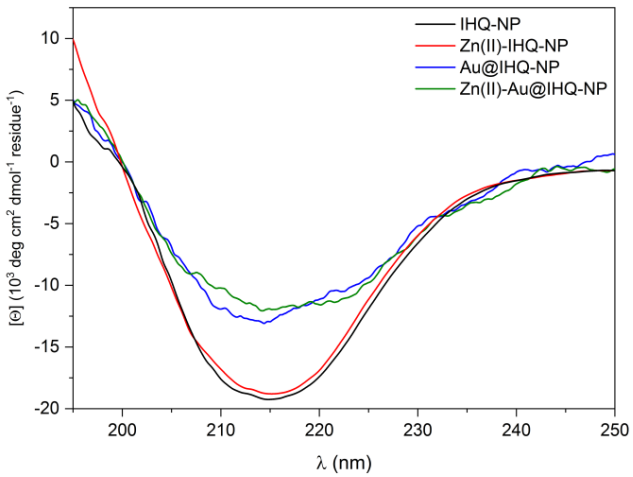

Figure 2. Circular dichroism (CD)-spectra of IHQ-NP and peptide–gold nanoparticle conjugates (Au@IHQ-NP) in absence or presence of Zn(II). CD-spectra were recorded in Tris/HCl buffer pH 8 with 5% acetonitrile at 25 °C in presence of 10 μM (immobilized) IHQ-NP and 100 μM $ZnCl_2$, when in presence of Zn(II).

2.2. Esterase Activity

Although the natural reaction catalyzed by CA is the reversible hydration of CO_2 to HCO_3^-, a frequently used benchmark reaction to study the successful coordination of Zn(II) and function of the active sites is the hydrolysis of model substrate 4-nitrophenyl acetate (4-NPA) [24]. Both reactions are initiated by a similar mechanism, that is, the nucleophilic attack of the Zn(II)-bound hydroxide to the substrate (Scheme 1) [25,26]. The hydrolysis of 4-NPA can readily be traced by measuring the UV/vis-absorbance of the 4-nitrophenolate (4-NP) product at 405 nm.

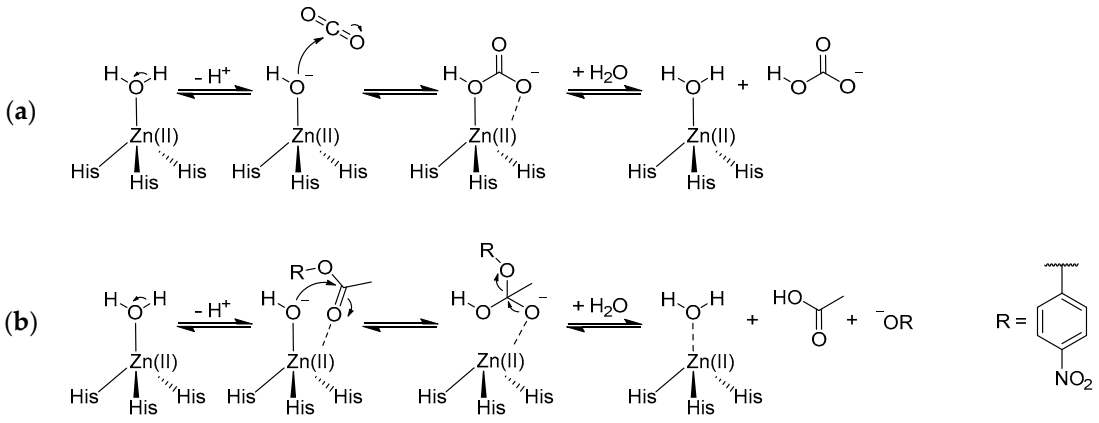

Scheme 1. Proposed reaction mechanisms of (**a**) CO_2-hydration and (**b**) 4-nitrophenyl acetate (4-NPA) hydrolysis initiated by the nucleophilic Zn(II)-bound hydroxide [26].

To verify the Zn(II)-binding and function of the catalytic Zn(II)-center, IHQ-NP and Au@IHQ-NP were studied in the context of their ability to cleave 4-NPA in absence or presence of Zn(II). In the absence of Zn(II) nucleophilic and/or general acid/base catalysis performed by the His imidazole is expected, while in presence of Zn(II), hydrolysis is executed by the more rapid Zn(II)-bound hydroxide mechanism [19].

To ensure proper metal coordination [19], 10 equivalents of Zn(II) were added to the catalyst mixture and the resulting Zn(II)-containing peptide(-gold nanoparticle conjugate) are referred to as Zn(II)-IHQ-NP and Zn(II)-Au@IHQ-NP.

Figure 3a,b show the blank-corrected saturation curves of IHQ-NP and Au@IHQ-NP in the presence or absence of Zn(II). While the dependence of unconjugated Zn(II)-/IHQ-NP-catalyzed 4-NPA hydrolysis on 4-NPA concentration displays hyperbolic behavior (Figure 3a), which is in accordance with the Michaelis–Menten theory, sigmoidal behavior was observed for Zn(II)-/Au@IHQ-NP (Figure 3b). A sigmoidal profile indicates a positive cooperative effect for the binding of substrate molecules among individual active sites and has been previously observed to be an effect evoked by the conjugation and the resulting high peptide density within the peptide monolayer [9,11]. Positive cooperativity in substrate binding is classified as a regulatory mechanism also found in nature. Instead of a linearly increasing behavior of the catalytic response curve at low substrate concentrations (0–0.1 mM), the ascent of the catalytic response curve starts shallow, as above a certain concentration, small changes in the substrate concentration lead to greater catalytic responses. The Hill-coefficient n is frequently used to express the magnitude of cooperativity or slope of the sigmoidal curve. We found positive cooperativity in Zn(II)-Au@IHQ-NP-catalyzed 4-NPA hydrolysis (n = 2.5) to be 0.6 units higher compared to Au@IHQ-NP (n = 1.9), indicating that Zn(II)-binding alters substrate interactions and the associated catalytic process.

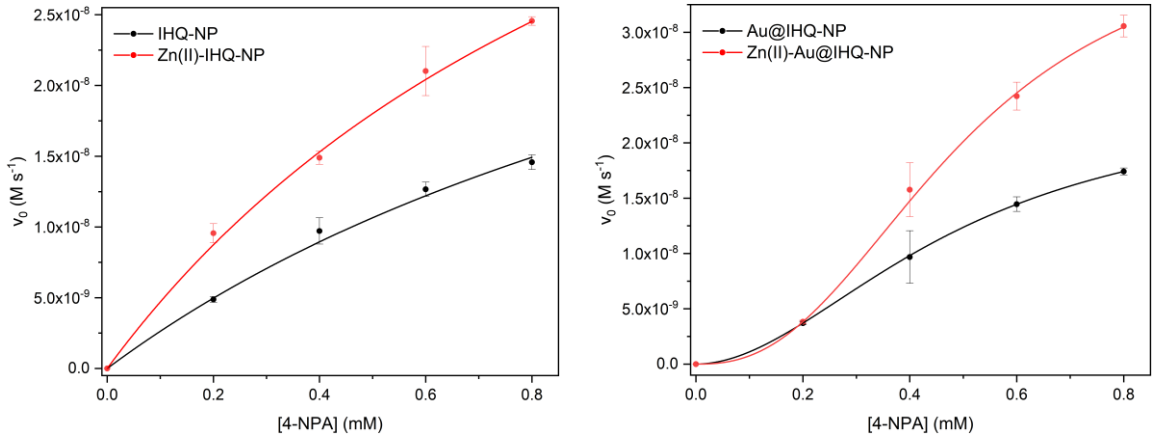

Figure 3. Saturation curves of background-corrected 4-NPA hydrolysis catalyzed by (**a**) IHQ-NP and (**b**) Au@IHQ-NP in absence and presence of Zn(II), respectively. Hydrolysis reactions were carried out in 50 mM Tris/HCl buffer pH 8 with 5% acetonitrile at 25 °C. (Immobilized) IHQ-NP concentration of 10 µM was used, while 100 µM $ZnCl_2$ was added for reactions in presence of Zn(II).

Table 1 summarizes the catalytic parameters k_{cat}, K_M, and k_{cat}/K_M of IHQ-NP, Au@IHQ-NP in the absence or presence of Zn(II). The immobilization of IHQ-NP onto the surface of Au-NPs (Au@IHQ-NP) led to an overall increase in catalytic efficiency (k_{cat}/K_M) by almost 2-fold. Interestingly, the increase in k_{cat}/K_M originates exclusively from a decrease in K_M, indicating a higher affinity for the peptide monolayer. We assume that the high peptide density leads to the formation of a secondary coordination sphere with sophisticated substrate interactions and possibly the formation of transient binding pockets within the peptide monolayer that lead to improved binding. Riccardi et al. previously verified the formation of such pockets for the binding of small molecules using even less complex Au-MPCs consisting of oligo(ethylene glycol)-based thiols [27]. Thus, it may be expected that Pep-Au-NPs composed of peptides with a more diverse set of functionalities are able to form similar binding cavities.

Table 1. Determined kinetic parameters k_{cat}, K_M, and k_{cat}/K_M of IHQ-NP-catalyzed 4-NPA hydrolysis in absence and presence of Zn(II). Reactions were performed in Tris/HCl buffer pH 8 with 5% acetonitrile at 25 °C 10 µM (Immobilized) IHQ-NP was used and 100 µM $ZnCl_2$ was added for reactions performed in presence of Zn(II).

Catalyst	k_{cat} (10^{-3} s^{-1})	K_M (mM)	k_{cat}/K_M (M^{-1} s^{-1})
IHQ-NP [1]	4.49 ± 0.68	1.61 ± 0.27	2.79 ± 0.98
Zn(II)-IHQ-NP [1]	10.53 ± 0.72	1.21 ± 0.20	8.69 ± 1.47
Au@IHQ-NP [2]	2.41 ± 0.02	0.49 ± 0.06	4.95 ± 0.61
Zn(II)-Au@IHQ-NP [2]	7.97 ± 0.41	0.50 ± 0.03	16.06 ± 1.78

[1] Parameter determined by fit to the Michaelis–Menten equation. [2] Parameter determined by fit to the Hill equation.

The addition of Zn(II) to the peptide catalysts further improved the catalytic efficiency for the Zn(II)-IHQ-NP- and Zn(II)-Au@IHQ-NP-catalyzed ester hydrolysis by more than 3-fold, compared to the respective peptides in the absence of Zn(II). This time, the improvement in catalytic efficiency of Zn(II)-IHQ-NP and Zn(II)-Au@IHQ-NP results from both a decrease in K_M and an increase in turnover number k_{cat} by 2- and 3-fold, respectively. The increase in catalytic activity upon addition of Zn(II) is in accordance with the rate enhancements reported for the IHQ peptide when the catalytic Zn(II)-center is developed [19]. Hence, IHQ-NP and Au@IHQ-NP are able to bind Zn(II) and execute

4-NPA hydrolysis by the Zn(II)-bound hydroxide mechanism rather than nucleophilic and/or general acid/base catalysis performed by the His imidazole.

Compared to other literature on known Pep-Au-NPs by Koksch and co-workers [9–11] or Pengo et al. [7,8], (Zn(II)-)Au@IHQ-NP shows only moderate catalytic efficiency. However, both particle size and peptide loading deviate from the reported conjugates and most probably influence the catalytic properties. Thus, comparisons of catalytic efficiency should be done carefully. Interestingly, independent of the conjugate, all show a similar K_M of approximately 0.5 mM [9–11], indicating a similar affinity of 4-NPA for the respective peptide monolayers.

2.3. Carbonic Anhydrase Activity

We were particularly interested in establishing Au@IHQ-NP as a catalyst for the hydration of CO_2 to HCO_3^-. Since H^+ is generated during the catalytic process, the chemical absorption of CO_2 can readily be monitored by following the change in pH over time, which is the basis for the frequently used delta-pH method [28–30]. Here, the delta-pH method serves as a qualitative tool to investigate the kinetics of CO_2-hydration and proof-of-concept for Au@IHQ-NP functioning as a CA mimic.

Kinetic experiments were conducted in Tris/HCl buffer pH 8.9 in order to sufficiently cover the drop in pH over 2 units of pH, in the absence or presence of Zn(II). Figure 4a shows the time-dependent change in pH during the hydration of CO_2 in presence of IHQ-NP and Au@IHQ-NP, compared to the buffer control.

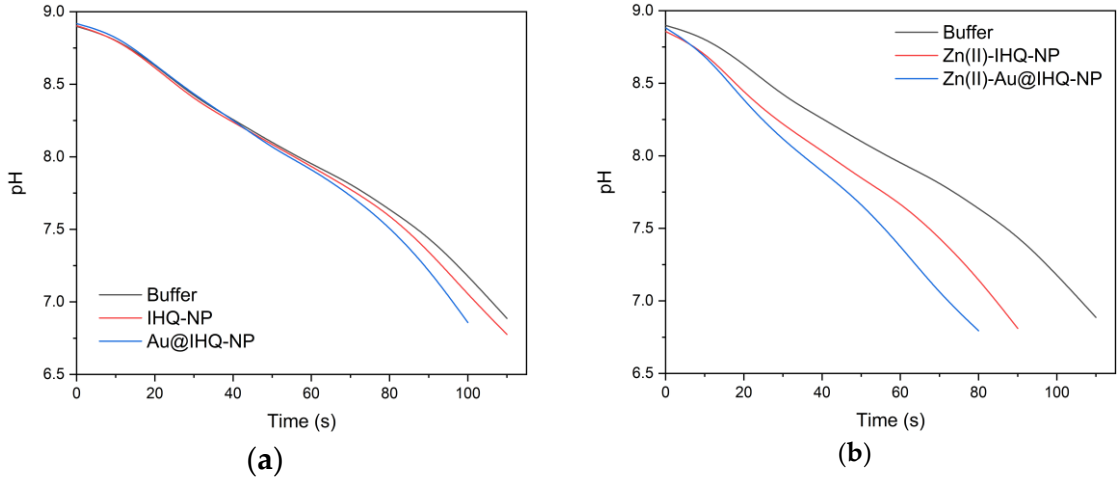

Figure 4. CO_2-hydration activity via delta-pH of IHQ-NP and Au@IHQ-NP in (**a**) the absence or (**b**) the presence of Zn(II). CO_2-hydration was performed in 50 mM Tris/HCl buffer pH 8.9 either in the absence of $ZnCl_2$ (**a**) or containing 100 µM $ZnCl_2$ (**b**). 10 µM (immobilized) IHQ-NP was used, while CO_2 flow rate was kept constant at 0.1 L/min.

Both, IHQ-NP and Au@IHQ-NP show a marginal drop in pH over the buffer control, thus marginal increases in CO_2 hydration in the absence of Zn(II) by ~3% and 6%, respectively. The small rate increase of IHQ-NP and Au@IHQ-NP can be attributed to the His imidazole which is reported to promote CO_2 hydration [31–33].

More strikingly, the pH drops significantly faster for Zn(II)-IHQ-NP and Zn(II)-Au@IHQ-NP, compared to the buffer control (Figure 4b). CO_2-hydration increases by 21% and 55%, respectively. The significantly higher activity in the presence of Zn(II) indicates that the catalytic process proceeds via the catalytic Zn(II)-center. Interestingly, Zn(II)-Au@IHQ-NP shows a significantly greater rate acceleration compared to the unconjugated Zn(II)-IHQ-NP. We assume that the peptide monolayer again acts as a more elaborate secondary coordination sphere in which CO_2 interactions and/or transition state stabilization take place. To date, increased rates of reaction, evoked solely by conjugation of a peptide to the surface of Au-NPs, has only been observed in ester hydrolysis reactions performed by a

His imidazole [7–11]. The herein described CO_2 hydration indicates that the cooperative or synergistic effects that lead to the rate improvements are also applicable to other reactions executed by catalytic (metal) centers. Moreover, we hypothesize that the introduced polar region at the solvent exposed end of the peptide monolayer facilitates water/H^+-shuttling as is the case in native CA. However, detailed mechanistic studies are necessary in order to elucidate the complex process that leads to the observed rate enhancements of Zn(II)-Au@IHQ-NP.

Since conjugation of peptides onto Au-NPs represents a transition from homogenous to heterogeneous catalysis, recycling of Zn(II)-Au@IHQ-NP is feasible. Subsequent to CO_2 hydration, we released the absorbed CO_2 by elevating the temperature of the reaction mixture to 60 °C and bubbling a stream of N_2-gas through the solution, until the initial pH of 8.9 was reached. We observed a slight change in the color of the Pep-Au-NP dispersion from red to violet, indicating some degree of instability of the Au-NPs. However, to our surprise, the treatment of the reaction mixture and subsequent color change did not affect the catalytic activity as Zn(II)-Au@IHQ-NP maintained almost 94% of its activity over five cycles of CO_2 hydration (Figure 5a,b).

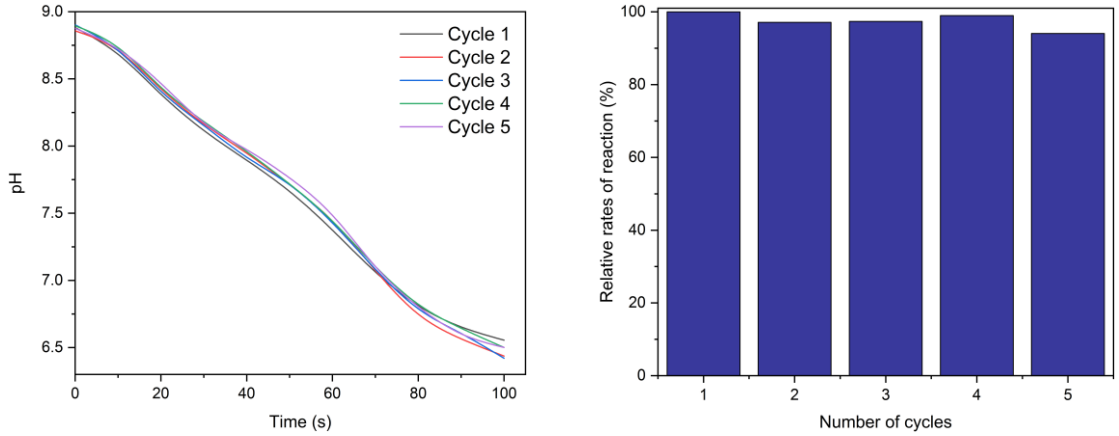

Figure 5. Reusability study of Zn(II)-Au@IHQ-NP for the catalyzed hydration of CO_2. (**a**) Delta-pH graphs of five cycles of CO_2 hydration. (**b**) Relative rates of reaction determined over 5 cycles of CO_2 hydration.

3. Materials and Methods

3.1. Peptide Synthesis

Peptide IHQ-NP were synthesized using microwave-assisted solid-phase peptide synthesis (Liberty Blue synthesizer, CEM Corporation, Matthews, NC, USA). The coupling of each Fmoc-protected amino acid (5 equivalents; ORPEGEN Peptide Chemicals GmbH, Heidelberg, Germany) was performed using reagents *N*,*N*′-diisoproplycarbodiimide (DIC; 4.9 equivalents) and ethyl 2-cyano-2-(hydroxyimino)acetate (Oxyma; 5 equivalents) obtained from Sigma-Aldrich® (Merck KGaA, Darmstadt, Germany) in *N*,*N*-Dimethylformamide (DMF, synthesis grade; Fisher Scientific, Schwerte, Germany). Cleavage of peptide from the resin (Fmoc-Lys preloaded TentaGel® S RAM Resin; Rapp Polymere GmbH, Tuebingen, Germany) as well as side-chain deprotection was performed by using a cleavage mixture of thioanisole, phenol, 1,2-ethanedithiol (EDT) obtained from Acros Organics (Thermo Fisher Scientific, Geel, Belgium), H_2O, and trifluoroacetic acid (TFA; Merck KGaA, Darmstadt, Germany) (5:5:2.5:2.5:85, v/v). Ice-cold diethyl ether was used to precipitate the crude peptides before purification by reverse-phase (RP) HPLC LaPrep∑ low-pressure HPLC system (VWR, Darmstadt, Germany) using a Kinetex RP-C18 end-capped HPLC-column (5 µM, 100 Å, 250 × 21.2 mm, Phenomenex®, Torrance, CA, USA). A SecurityGuard™ PREP Cartridge Holder Kit (21.20 mm, ID, Phenomenex®, Torrance, CA, USA) was used as pre-column. Deionized water (Milli-Q Advantage®

A10 Ultrapure Water Purification System, Millipore®, Billerica, MA, USA) and acetonitrile (can, analytical grade; Fisher Scientific, Schwerte, Germany), both containing 0.1% (v/v) TFA, were used as eluents. HPLC runs were performed with a linear gradient of 5–70% ACN over 25 min, flow rate: 15.0 mL/min.

3.2. Peptide Stock Solution

Amyloidogenic IHQ-NP was handled according to Rufo et al. [19]. Briefly, IHQ-NP stock solution was prepared by dissolving lyophilized IHQ-NP in 10 mM HCl. Concentration of stock solution was determined by using a Varian Cary 50 UV-Vis Spectrophotometer (Agilent Technologies, Santa Clara, CA, USA) and by applying an experimentally determined extinction coefficient (ε_{280}) of 1263 L mol^{-1} cm^{-1}. Working solutions at elevated pH >8 were freshly prepared and the pH verified before each individual measurement.

3.3. Synthesis of Au@IHQ-NP

Pep-Au-NP synthesis was performed according to our previously established procedure [10]. Briefly, an aqueous solution of $HAuCl_4$ (0.8 mL, 2.49 × 10^{-2} M; Sigma-Aldrich®, Merck KGaA, Darmstadt, Germany) was added to enzyme-free water (EF-H_2O; Water for Molecular Biology, Merck KGaA, Darmstadt, Germany) containing IHQ-NP (1.5 mL of 0.6 mM Solution) while carefully adjusting the pH to a value of 6 (total reaction volume 10 mL). Slightly acidic reaction conditions prevented premature aggregation of the peptide. An aqueous solution of freshly prepared $NaBH_4$ (0.3 mL, 0.01 M) was added after 5 min of stirring. Following an additional 1 h of vigorous stirring, the formed red dispersion was centrifuged using centrifugal filters (Amicon Ultra-0.5 NMWL 30 kDa; Sigma-Aldrich®, Merck KGaA, Darmstadt, Germany) to recover Au@IHQ-NP as a dark red pellet. The pellet was redispersed in EF-H_2O and again centrifuged to remove excess $NaBH_4$. The resulting pellet was redispersed in EF-H_2O and stored at room temperature. Nanoparticle concentration was calculated according to equations provided by Liu et al. [34]. The average peptide loading was determined by supernatants as previously described [9,10]. Briefly, after centrifugation, the supernatant was analyzed and the amount of unbound peptide determined by UV/vis-spectroscopy (see Section 3.2). The amount of unbound peptide was subtracted from the amount of peptide added during the reaction, giving the amount of bound peptide on the Au-NPs.

3.4. Esterase Activity

The rates of hydrolysis of 4-NPA were monitored in 50 mM Tris/HCl pH 8 at a constant temperature of 25 °C by measuring the UV/vis-absorbance at 405 nm of the formed product 4-nitrophenolate (4-NP). Using a literature-reported extinction coefficient of 16,600 L mol^{-1} cm^{-1} [19], initial rates of reaction (v_0) of uncatalyzed (blank) and catalyzed reactions were determined over a range of substrate concentrations until saturation conditions were observed. Initial rates of reaction of the catalysts were obtained by subtracting v_0 of the blank reactions from v_0 of the corresponding catalyzed reaction. Kinetic experiments were performed at least three times to determine standard deviations. The Kinetic parameters v_{max}, K_M, and the Hill-coefficient *n* were obtained by fitting the measured data points to the Hill or Michaelis–Menten equation by performing a nonlinear regression using OriginLab (OriginPro, Version 2019 Academic; OriginLab Corporation, Northampton, MA, USA.) Calculation of errors and error propagation was carried out according to Gaussian equations for normally distributed errors and the derived error propagation.

Ester hydrolysis was performed in quartz cuvettes (QS, 1 cm path length 3.5 mL, Hellma Analytics) using Varian Cary 50 UV-Vis Spectrophotometer (Agilent Technologies, Santa Clara, CA, USA) thermostatted at 25 °C (Lauda RKS). Ester hydrolysis was initiated by addition of a defined volume of 4-NPA stock solution in acetonitrile. In total, 5% acetonitrile was present in each reaction mixture.

Kinetic studies were conducted using a calculated (immobilized) peptide concentration of 10 μM, while 100 μM $ZnCl_2$ was added when the reaction mixture contained Zn(II). Initial 4-NPA concentration was gradually increased so 0.2, 0.4, 0.6, and 0.8 mM were applied in 4-NPA hydrolysis.

3.5. Carbonic Anhydrase Activity

The delta-pH method was used to determine the feasibility of peptide/Pep-Au-NP-catalyzed CO_2 hydration. A setup reported by Kellsey et al. was modified and used for all hydration reactions [29]. Briefly, a pH probe and glass tubing were immersed into the two necks of a 2-necked 100 mL round-bottom flask containing 10 μM of the respective (immobilized) IHQ-NP in the absence and presence of 100 μM $ZnCl_2$ in Tris/HCl-buffer pH 8.9 (total volume 40 mL) at 22 °C. CO_2 gas (Carbon dioxide N35, Air Liquide) was streamed through the gas tubing into the reaction mixture at a constant flow of 0.1 L/min. The changes in pH were recorded automatically using a pHenomenal® pH 1100L pH-meter (VWR International GmbH, Darmstadt, Germany). Rates of hydration were determined by the slope of the plot of time-dependent pH changes.

4. Conclusions

In summary, the catalytically active Zn(II)-binding peptide IHQ-NP was conjugated onto Au-NPs leading to the formation of a peptide monolayer that is able to bind Zn(II) and develop a catalytic Zn(II)-center. Peptide variants IHQ-NP and Au@IHQ-NP were tested for their ability to serve as esterase and carbonic anhydrase mimics. While IHQ-NP and Au@IHQ-NP both noticeably catalyze ester hydrolysis and marginally catalyze CO_2 hydration in the absence of Zn(II), significant improvements in catalytic efficiency and rate acceleration were observed in the presence of Zn(II) for both reactions. The Zn(II)-Au@IHQ-NP showed even greater rate improvements for ester hydrolysis and CO_2 hydration compared to the unconjugated Zn(II)-IHQ-NP variant. This is in accordance with previously reported results showing that Pep-Au-NPs can generate secondary coordination spheres in which synergistic effects and cooperativity in substrate binding and the associated improvements in catalysis over the unconjugated peptide are observed. Recycle experiments further revealed Zn(II)-Au@IHQ-NP to maintain at least 94% of its catalytic activity over 5 cycles of CO_2 hydration. Altogether, the herein reported results validate the proof-of-concept that Pep-Au-NPs can be designed to bind metal ions within their peptide monolayer and develop metalloenzymatic activities. The presented results provide a design principle based on a well-defined peptide secondary structure and demonstrate the exponentially increasing possibilities, due to the combination of Au-NPs and catalytically active peptide sequences, as their catalytic toolbox can be further expanded based on nature's examples.

Supplementary Materials: The following are available online at http://www.mdpi.com/2073-4344/9/11/903/s1; Experimental procedures of CD-, IR-, and UV/vis-spectroscopy and respective spectra. Calculation of gold nanoparticle concentration. TEM preparation and micrographs.

Author Contributions: Conceptualization, D.J.M. and B.K.; methodology, D.J.M. and B.K.; formal analysis, D.J.M. and B.K.; investigation, D.J.M.; writing—original draft preparation, D.J.M.; writing—review and editing, B.K.; visualization, D.J.M.; supervision, B.K.

Funding: This research received no external funding.

Acknowledgments: The publication of this article was funded by Freie Universität Berlin. The authors thank Dr. Allison A. Berger (Koksch group, FU Berlin) for critical reading and fruitful discussions that improved the manuscript. The authors also thank the German Federal Environmental Foundation (Deutsche Bundesstiftung Umwelt, DBU), as well as the Integrated Research Training Group "Multivalency in Chemistry and Biochemistry" of the Collaborative Research Center 765 (SFB 765) "Multivalency as Chemical Organizational and Operational Principle: New Architectures, Functions, and Applications" at the Freie Universitaet Berlin funded by the German Research Foundation (DFG) for financial support. We also would like to acknowledge the assistance of the Core Facility BioSupraMol supported by the DFG.

Conflicts of Interest: The authors declare no conflict of interest.

References

1. Pasquato, L.; Pengo, P.; Scrimin, P. Nanozymes: Functional Nanoparticle-Based Catalysts. *Supramol. Chem.* **2005**, *17*, 163–171. [CrossRef]
2. Wang, X.; Hu, Y.; Wei, H. Nanozymes in Bionanotechnology: From Sensing to Therapeutics and Beyond. *Inorg. Chem. Front.* **2016**, *3*, 41–60. [CrossRef]
3. Singh, S. Catalytically Active Nanomaterials: Artificial Enzymes of Next Generation. *Nanosci. Technol.* **2017**, *5*, 1–6. [CrossRef]
4. Wei, H.; Wang, E. Nanomaterials with Enzyme-like Characteristics (Nanozymes): Next-Generation Artificial Enzymes. *Chem. Soc. Rev.* **2013**, *42*, 6060–6093. [CrossRef]
5. Lin, Y.; Ren, J.; Qu, X. Nano-Gold as Artificial Enzymes: Hidden Talents. *Adv. Mater.* **2014**, *26*, 4200–4217. [CrossRef]
6. Pasquato, L.; Pengo, P.; Scrimin, P. Functional Gold Nanoparticles for Recognition and Catalysis. *J. Mater. Chem.* **2004**, *14*, 3481–3487. [CrossRef]
7. Pengo, P.; Polizzi, S.; Pasquato, L.; Scrimin, P. Carboxylate-Imidazole Cooperativity in Dipeptide-Functionalized Gold Nanoparticles with Esterase-like Activity. *J. Am. Chem. Soc.* **2005**, *127*, 1616–1617. [CrossRef]
8. Pengo, P.; Baltzer, L.; Pasquato, L.; Scrimin, P. Substrate Modulation of the Activity of an Artificial Nanoesterase Made of Peptide-Functionalized Gold Nanoparticles. *Angew. Chem. Int. Ed.* **2007**, *46*, 400–404. [CrossRef]
9. Mikolajczak, D.J.; Koksch, B. Peptide-Gold Nanoparticle Conjugates as Sequential Cascade Catalysts. *ChemCatChem* **2018**, 4324–4328. [CrossRef]
10. Mikolajczak, D.J.; Heier, J.L.; Schade, B.; Koksch, B. Catalytic Activity of Peptide-Nanoparticle Conjugates Regulated by a Conformational Change. *Biomacromolecules* **2017**, *18*, 3557–3562. [CrossRef]
11. Mikolajczak, D.J.; Scholz, J.; Koksch, B. Tuning the Catalytic Activity and Substrate Specificity of Peptide-Nanoparticle Conjugates. *ChemCatChem* **2018**, *10*, 5665–5668. [CrossRef]
12. McCall, K.A.; Huang, C.; Fierke, C.A. Function and Mechanism of Zinc Metalloenzymes. *J. Nutr.* **2000**, *130*, 1437S–1446S. [CrossRef] [PubMed]
13. Zastrow, M.L.; Pecoraro, V.L. Designing Hydrolytic Zinc Metalloenzymes. *Biochemistry* **2014**, *53*, 957–978. [CrossRef] [PubMed]
14. Christianson, D.W.; Fierke, C.A. Carbonic Anhydrase: Evolution of the Zinc Binding Site by Nature and by Design. *Acc. Chem. Res.* **1996**, *29*, 331–339. [CrossRef]
15. Boone, C.D.; Habibzadegan, A.; Gill, S.; Mckenna, R. Carbonic Anhydrases and Their Biotechnological Applications. *Biomolecules* **2013**, *3*, 553–562. [CrossRef] [PubMed]
16. Boone, C.D.; Gill, S.; Habibzadegan, A.; McKenna, R. Carbonic Anhydrase: An Efficient Enzyme with Possible Global Implications. *Int. J. Chem. Eng.* **2013**, 1–6. [CrossRef]
17. Yong, J.K.J.; Stevens, G.W.; Caruso, F.; Kentish, S.E. The Use of Carbonic Anhydrase to Accelerate Carbon Dioxide Capture Processes. *J. Chem. Technol. Biotechnol.* **2015**, *90*, 3–10. [CrossRef]
18. Mirjafari, P.; Asghari, K.; Mahinpey, N. Investigating the Application of Enzyme Carbonic Anhydrase for CO_2 Sequestration Purposes. *Ind. Eng. Chem. Res.* **2007**, *46*, 921–926. [CrossRef]
19. Rufo, C.M.; Moroz, Y.S.; Moroz, O.V.; Stöhr, J.; Smith, T.A.; Hu, X.; DeGrado, W.F.; Korendovych, I.V. Short Peptides Self-Assemble to Produce Catalytic Amyloids. *Nat. Chem.* **2014**, *6*, 303–309. [CrossRef]
20. Un, C.; Song, H.; Sankara, B.; Gruner, S.M.; Park, S.; Mckenna, R. Tracking Solvent and Protein Movement during CO_2 Release in Carbonic Anhydrase II Crystals. *Proc. Natl. Acad. Sci. USA* **2016**, *113*, 5257–5262. [CrossRef]
21. Mikulski, R.L.; Silverman, D.N. Proton Transfer in Catalysis and the Role of Proton Shuttles in Carbonic Anhydrase. *Biochim. Biophys. Acta Proteins Proteom.* **2010**, *1804*, 422–426. [CrossRef] [PubMed]
22. Colangelo, E.; Chen, Q.; Davidson, A.M.; Paramelle, D.; Sullivan, M.B.; Volk, M.; Levy, R. Experimental and Computational Investigation of the Structure of Peptide Monolayers on Gold Nanoparticles. *Langmuir* **2017**, *33*, 438–449. [CrossRef] [PubMed]
23. Shaw, C.P.; Middleton, D.A.; Volk, M.; Lévy, R. Amyloid-Derived Peptide Forms Self-Assembled Monolayers on Gold Nanoparticle with a Curvature-Dependent β-Sheet Structure. *ACS Nano* **2012**, *6*, 1416–1426. [CrossRef] [PubMed]

24. Uda, N.R.; Seibert, V.; Stenner-Liewen, F.; Müller, P.; Herzig, P.; Gondi, G.; Zeidler, R.; van Dijk, M.; Zippelius, A.; Renner, C. Esterase Activity of Carbonic Anhydrases Serves as Surrogate for Selecting Antibodies Blocking Hydratase Activity. *J. Enzyme Inhib. Med. Chem.* **2015**, *30*, 955–960. [CrossRef]
25. Zastrow, M.L.; Peacock, A.F.A.; Stuckey, J.A.; Pecoraro, V.L. Hydrolytic Catalysis and Structural Stabilization in a Designed Metalloprotein. *Nat. Chem.* **2011**, *4*, 118–123. [CrossRef]
26. Gould, S.M.; Tawfik, D.S. Directed Evolution of the Promiscuous Esterase Activity of Carbonic Anhydrase II. *Biochemistry* **2005**, *44*, 5444–5452. [CrossRef]
27. Riccardi, L.; Gabrielli, L.; Sun, X.; De Biasi, F.; Rastrelli, F.; Mancin, F.; De Vivo, M. Nanoparticle-Based Receptors Mimic Protein-Ligand Recognition. *Chem* **2017**, *3*, 92–109. [CrossRef]
28. Lippert, C.A.; Liu, K.; Sarma, M.; Parkin, S.R.; Remias, J.E.; Brandewie, C.M.; Odom, S.A.; Liu, K. Improving Carbon Capture from Power Plant Emissions with Zinc- and Cobalt-Based Catalysts. *Catal. Sci. Technol.* **2014**, *4*, 3620–3625. [CrossRef]
29. Kelsey, R.A.; Miller, D.A.; Parkin, S.R.; Liu, K.; Remias, J.E.; Yang, Y.; Lightstone, F.C.; Liu, K.; Lippert, C.A.; Odom, S.A. Carbonic Anhydrase Mimics for Enhanced CO_2 Absorption in an Amine-Based Capture Solvent. *Dalt. Trans.* **2016**, *45*, 324–333. [CrossRef]
30. Bond, G.M.; Stringer, J.; Brandvold, D.K.; Simsek, F.A.; Medina, M.-G.; Egeland, G. Development of Integrated System for Biomimetic CO_2 Sequestration Using the Enzyme Carbonic Anhydrase. *Energy Fuels* **2001**, *15*, 309–316. [CrossRef]
31. Muñoz, D.M.; Portugal, A.F.; Lozano, A.E.; de la Campa, J.G.; de Abajo, J. New Liquid Absorbents for the Removal of CO_2 from Gas Mixtures. *Energy Environ. Sci.* **2009**, *2*, 883–891. [CrossRef]
32. Tomizaki, K.; Kanakubo, M.; Nanjo, H.; Shimizu, S.; Onoda, M.; Fujioka, Y. 13C NMR Studies on the Dissolution Mechanisms of Carbon Dioxide in Amine-Containing Aqueous Solvents at High Pressures toward an Integrated Coal Gasification Combined Cycle−Carbon Capture and Storage Process. *Ind. Eng. Chem. Res.* **2010**, *49*, 1222–1228. [CrossRef]
33. Evjen, S.; Fiksdahl, A.; Pinto, D.D.D.; Knuutila, H.K. New Polyalkylated Imidazoles Tailored for Carbon Dioxide Capture. *Int. J. Greenh. Gas Control* **2018**, *76*, 167–174. [CrossRef]
34. Liu, X.; Atwater, M.; Wang, J.; Huo, Q. Extinction Coefficient of Gold Nanoparticles with Different Sizes and Different Capping Ligands. *Colloids Surf. B Biointerfaces* **2007**, *58*, 3–7. [CrossRef]

© 2019 by the authors. Licensee MDPI, Basel, Switzerland. This article is an open access article distributed under the terms and conditions of the Creative Commons Attribution (CC BY) license (http://creativecommons.org/licenses/by/4.0/).